

Vortex patterns in a superconducting-ferromagnetic rod

Antonio R. de C. Romaguera^a, Mauro M. Doria^b, François M. Peeters^c

^a*Departamento de Física, Universidade Federal Rural de Pernambuco,
52171-900 Recife, Pernambuco, Brazil*

^b*Departamento de Física dos Sólidos, Universidade Federal do Rio de Janeiro,
21941-972 Rio de Janeiro, Brazil*

^c*Departement Fysica, Universiteit Antwerpen,
Groenenborgerlaan 171, B-2020 Antwerpen, Belgium*

Abstract

A superconducting rod with a magnetic moment on top develops vortices obtained here through 3D calculations of the Ginzburg-Landau theory. The inhomogeneity of the applied field brings new properties to the vortex patterns that vary according to the rod thickness. We find that for thin rods (disks) the vortex patterns are similar to those obtained in presence of a homogeneous magnetic field instead because they consist of giant vortex states. For thick rods novel patterns are obtained as vortices are curve lines in space that exit through the lateral surface.

Key words: Vortex pattern, Ginzburg-Landau, Magnetic dot

PACS: 74.20.-z, 74.20.De

1. Introduction

The minimal condition for the onset of a vortex in a mesoscopic superconductor depends on geometrical parameters. A thin disk of radius R (thickness $D \sim \xi$, ξ is the coherence length) can only exist in the Meissner state for $R \sim \xi$. But for $\xi < R < 2\xi$, giant vortex states are allowed and for $R > 2\xi$ multivortex states become possible, as reported in [1] and recently observed in Refs. [2, 3]. Mesoscopic superconductors have new and interesting properties[4], and also provide an interesting playground to understand the co-existence of magnetism and superconductivity [5, 6]. For instance magnetic dots on top of superconducting film have been investigated both theoretically and experimentally [7–10].

In this paper we report a theoretical study done on superconducting rods of radius R and varying thickness D , with a magnetic dot on top, a system which displays curved vortices triggered by the inhomogeneity of the magnetic field. We address the minimal geometrical conditions for the

onset of vortices and also the nature of the vortex patterns.

The shape of a vortex shifts from a flat coin to a curved line in three-dimensional space, as the thickness D takes the rod from a disk to a tall rod. Consequently the vortex pattern consists of top to bottom giant vortices and top to side multi-vortices in these two extreme limits, namely, $D \sim \xi$ and $D \gg \xi$, respectively. Rods of intermediate thickness display highly non trivial

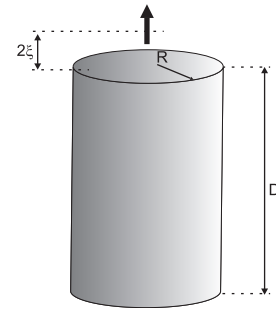


Figure 1: (Color online) Superconducting rod with radius R and thickness D . The magnetic dot is oriented along the x -axis and positioned 2ξ above the top surface.

vortex patterns showing features of both extreme limits. Our results are obtained in the context of the Ginzburg-Landau theory in the limit of no magnetic shielding. We take a magnetic dot with magnetic moment μ positioned 2ξ above the rod's top surface and oriented along the rod's axis, see Fig. 1.

Although curve vortices also appear in presence of a homogeneous field tilted with respect to the surface, as vortices must always emerge perpendicular to the surface [11], the inhomogeneity of the field brings new effects. The dipolar magnetic field weakens with distance and may become so dim at the bottom of the rod to the point that this region becomes unable to sustain vortices. Consequently the Meissner state is kept at the bottom of the rod. This favors a reentrant vortex state, as a top to side vortex must disappear at the top surface, the same one of its onset. Thus the Meissner phase is retrieved at a higher magnetic moment. This qualifies superconducting rods with a magnetic moment on top for technological applications as logical switchers, since vortices can be expelled or accepted by fine tuning the external magnetic moment dot strength.

2. Theoretical approach

According to the standard Ginzburg-Landau approach, the Gibbs free energy of the superconductor near the critical temperature T_c can be expanded in powers of the complex order parameter $\Psi(\vec{r})$ that gives the density of Cooper-pairs: $|\Psi(\vec{r})|^2$. Hence the Gibbs free energy difference between the superconducting and the normal states is,

$$F_s - F_n = \int dV \left\{ \alpha(T) |\Psi|^2 + \frac{1}{2} \beta |\Psi|^4 + \frac{\hbar^2}{2m^*} \left| \left(\vec{\nabla} - i \frac{2\pi}{\Phi_0} \vec{A} \right) \Psi \right|^2 \right\}$$

with the phenomenological constants $\alpha(T) \equiv \alpha_0(T - T_c) < 0$, $\beta > 0$, m^* (the mass of one Cooper-pair), and $\Phi_0 = hc/2e$, the fundamental unit of flux. Boundary conditions are imposed to the external surfaces of the rod. We express quantities in this theory in dimensionless units defined

by the following reduced units: the coherence length $\xi(T) = [-\hbar^2/2m^*\alpha(T)]^{1/2}$ (lengths), $H_{c2} = \phi_0/2\pi\xi(T)^2$ (magnetic field), $H_{c2}\xi = \Phi_0/2\pi\xi(T)$ (vector potential), $\mu_0 = H_{c2}\xi(T)^3 = \Phi_0\xi(T)/2\pi$ (magnetic moment), $\Psi_0 = \sqrt{-\alpha(T)/\beta}$ (order parameter), and $F_0 = \alpha(T)^2/2\beta$ (free energy). The magnetization is calculated using the expression $\vec{M} = \int \vec{r} \times \vec{J}(r) dv$.

In terms of these dimensionless units, the Gibbs free energy difference becomes,

$$F = 2 \int dV \left\{ -|\Psi|^2 + \frac{1}{2} |\Psi|^4 + |(\vec{\nabla} - i\vec{A})\Psi|^2 \right\}, \quad (1)$$

The integration is restricted to the volume of the rod. The boundary condition in dimensionless units becomes,

$$\vec{n} \cdot (\vec{\nabla} - i\vec{A})\Psi \Big|_{\text{boundary}} = 0. \quad (2)$$

For the magnetic dot we use field produced by a point-like dipole $\vec{A} = (\vec{\mu} \times \vec{r})/r^3$.

3. Numerical results

We solved Eqs. 1 and 2 using the simulated annealing procedure [4]. We set the following parameters for the rod: the radius R ranges from 1ξ to 4ξ ; the thickness D ranges from 2ξ to 8ξ and the magnetic moment μ ranges from 0 to $100\mu_0$. For the thinnest rod considered here, $D = 2\xi$, we find that the inhomogeneity of the field does not matter, since the free energy and the magnetization are similar to the homogeneous applied field case. Clearly this is because the dot's magnetic field does not vary significantly inside the rod.

For $R = 1\xi$ and any thickness we find no vortex state, thus the Meissner state prevails up to the normal state. We do not observe anti-vortices or Meissner state with opposite orientation in the rods because we limit the present study to rods with a maximum radius of 4ξ . Thus only giant vortex states (GVS) are observed. For $R = 2\xi$ and for $D = 2\xi$, only one vortex is allowed. For larger R more than one vortex is possible and their number increases very rapidly with the radius. Although there is more space to accommodate extra vortices the magnetic field becomes

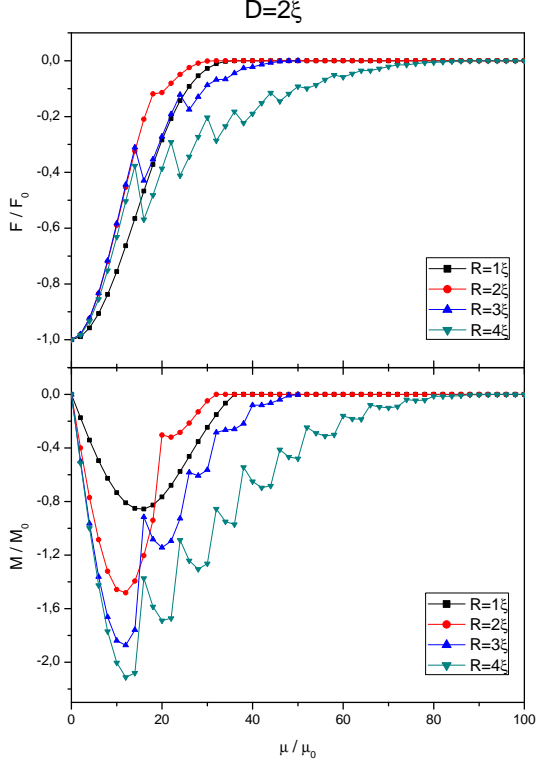


Figure 2: (Color online) Free energy F/F_0 and magnetization M/M_0 versus magnetic moment μ/μ_0 for mesoscopic rods with thickness $D = 2\xi$ and several radii. Giant vortices with increasing maximum vorticity are observed by increasing the radius.

weaker at distances away from the center. Consequently the average magnetic field does not grow with the radius. This effect is equivalent to that studied by Ovchinnikov sometime ago [12]. A sawtooth behavior in the magnetization with bigger H_{c2} is clearly established for bigger radius. This behavior is observed for $R = 3\xi$ and $D = 2\xi$. In Fig. 2 we show the vortex states obtained for different thin rods, i.e., disks. Their magnetization curves are similar to those obtained in presence of homogeneous field. In table 1 we give the complete description of the states through the set of parameters $(R, D, \mu/\mu_0)$.

The inhomogeneity of the field becomes important for the thicker rods $D = 6\xi$ and 8ξ , as shown here. Even for small radii, the rod already displays behavior that differs significantly from the homogeneous field case. We find smooth free energy lines, with no first order transition occasioned by the entrance of quantized vortex lines.

Fig. 3 shows the free energy for the $R = 4\xi$ and $D = 6\xi$ rod.

The 3D view of the Cooper pair density, $|\psi|^2$, shows curved top-to-side vortices, that is, vortices that enter from the top surface and exit perpendicularly in the side surface. We call them N-fold states, where N describes the number of vortices. Along the energy curve vs μ in Fig. 3 the states are labeled according to this definition. The N-fold states are not clearly seen in Fig. 3 because their free energy lines is superposed to the Meissner line from where is their onset and disappearance. However these states are clearly seen to exist by analyzing the $|\psi|^2$ isosurface, as shown in Fig. 4. In the two biggest rods considered here we observed the nucleation of N-fold states followed by Meissner and GVS. This features are justified by the growth of a normal region closer to the the magnetic dot position. When this normal region occupies a significant part of the rod the remaining superconducting part behaves as a thin rod, i.e., it does not exhibits N-fold states. So, we retrieve the Meissner state. This feature is in Table 1 and correspond to the second Meissner state.

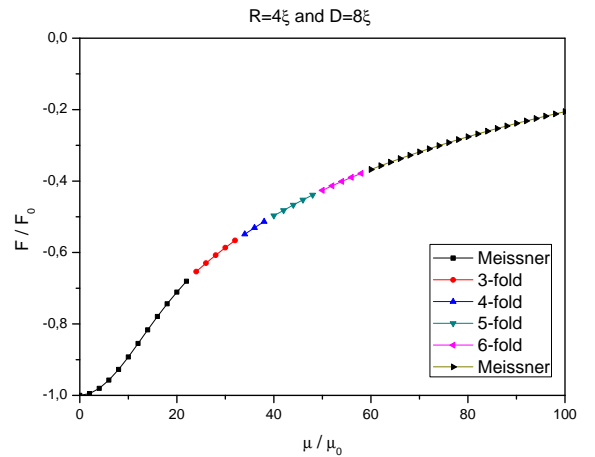


Figure 3: (Color online) Free energy F/F_0 vs μ/μ_0 for a rod with $R = 4\xi$ and $D = 8\xi$. For increasing magnetic moment the vortex pattern evolves continuously through the N-fold configurations, as labeled in the inset. See, Fig. 4 for the corresponding $|\psi|^2$ isosurface views of these N-fold states.

Table 1: The sequence of ground states for the rods considered here. The magnetic dot is positioned 2ξ away from the rod's top surface and oriented along the z -axis. The question mark means the normal state was not reach.

R/ξ	1	1	1	1	2	2	2	2	3	3	3	3	4	4	4	4
D/ξ	2	4	6	8	2	4	6	8	2	4	6	8	2	4	6	8
State	μ/μ_0	μ/μ_0	μ/μ_0	μ/μ_0	μ/μ_0	μ/μ_0	μ/μ_0	μ/μ_0	μ/μ_0	μ/μ_0	μ/μ_0	μ/μ_0	μ/μ_0	μ/μ_0	μ/μ_0	μ/μ_0
Meissner	0-36	< 100	< 100	< 100	0-18	0-76	< 100	< 100	0-14	0-46	< 100	< 100	0-14	0-20	0-22	0-22
1 GVS	-	-	-	-	20-30	78-100	-	-	16-24	48-76	-	-	16-22	22-100	-	-
2 GVS	-	-	-	-	32	-	-	-	26-30	78-100	-	-	24-30	-	-	-
3 GVS	-	-	-	-	-	-	-	-	32-38	-	-	-	32-36	-	-	-
4 GVS	-	-	-	-	-	-	-	-	40-50	-	-	-	38-44	-	-	-
5 GVS	-	-	-	-	-	-	-	-	-	-	-	-	46-50	-	-	-
3-fold	-	-	-	-	-	-	-	-	-	-	-	-	-	34-38	24-34	24-32
4-fold	-	-	-	-	-	-	-	-	-	-	-	-	-	40-44	36-42	34-40
5-fold	-	-	-	-	-	-	-	-	-	-	-	-	-	46-52	44-48	42-48
6-fold	-	-	-	-	-	-	-	-	-	-	-	-	-	54-56	50-54	50-58
7-fold	-	-	-	-	-	-	-	-	-	-	-	-	-	-	56-62	-
Meissner	-	-	-	-	-	-	-	-	-	-	-	-	-	-	64-74	60-100
1 GVS	-	-	-	-	-	-	-	-	-	-	-	-	-	-	76-100	-
Normal	> 36	?	?	?	> 32	?	?	?	> 50	?	?	?	?	?	?	?

4. Conclusions

Using Simulated Annealing, a truly three-dimensional approach, we obtain the vortex patterns of mesoscopic rods with a point-like magnetic moment on top. We conclude that rods with thickness smaller than 4ξ can be considered as thin disks since only top to bottom giant vortex states are obtained. For rods with thickness bigger than 4ξ , we observed the appearance of N-fold vortex states, namely N top-to-side vortices. The onset and disappearance of these states is from a single GVS or Meissner state line, as continuous transitions from it. Consequently, for sufficient large magnetic moments one can retrieve the Meissner state before reaching the normal state, and this, leads to a reentrant behavior.

5. Acknowledgment

A. R. de C. Romaguera acknowledges the brazilian agency FACEPE for financial support. M. M. Doria acknowledges CNPq and FAPERJ. F. M. Peeters acknowledges Flemish Science Foundation (FWO-VI), the Belgian Science Policy (IUAP) and the ESF-AQDJJ network.

References

- [1] B. J. Baelus, F. M. Peeters, V. A. Schweigert, Phys. Rev. B 63 (14) (2001) 144517.
- [2] I. V. Grigorieva, W. Escoffier, J. Richardson, L. Y. Vinnikov, S. Dubonos, V. Oboznov, Phys. Rev. Lett. 96 (7) (2006) 077005.
- [3] A. Kanda, B. J. Baelus, F. M. Peeters, K. Kadowaki, Y. Ootuka, Phys. Rev. Lett. 93 (25) (2004) 257002.

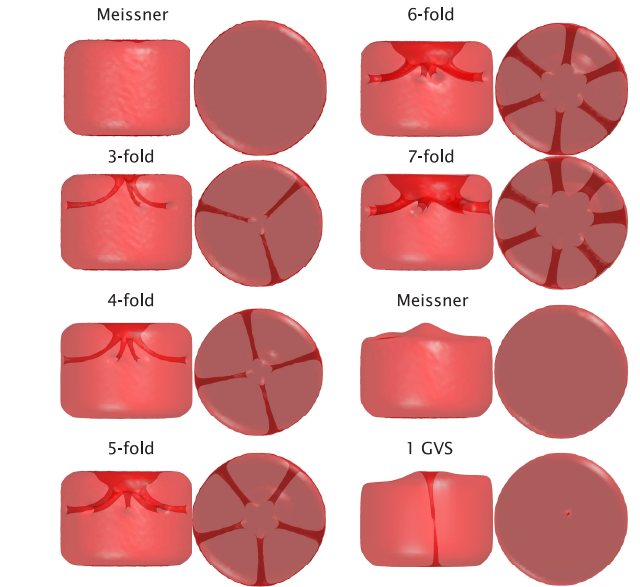


Figure 4: (Color online) Isosurfaces of the Cooper pair density for a mesoscopic rod with $R = 4\xi$ and $D = 6\xi$. Every image corresponds to one of the states N-fold states listed in Table 1.

- [4] A. R. de C. Romaguera, M. M. Doria, F. M. Peeters, Phys. Rev. B 76 (2) (2007) 020505.
- [5] M. V. Milošević, G. R. Berdiyrov, F. M. Peeters, Phys. Rev. B 75 (5) (2007) 052502.
- [6] Z. Yang, M. Lange, A. Volodin, R. Szymczak, V. V. Moshchalkov, Nature Material 3 (2004) 793.
- [7] M. J. Van Bael, K. Temst, V. V. Moshchalkov, Y. Bruynseraede, Phys. Rev. B 59 (22) (1999) 14674.
- [8] D. G. Gheorghe, R. J. Wijngaarden, W. Gillijns, A. V. Silhanek, V. V. Moshchalkov, Phys. Rev. B 77 (5) (2008) 054502.
- [9] A. Y. Aladyshkin, D. A. Ryzhov, A. V. Samokhvalov, D. A. Savinov, A. S. Mel'nikov, V. V. Moshchalkov, Phys. Rev. B 75 (18) (2007) 184519.
- [10] M. M. Doria, A. R. de C. Romaguera, F. M. Peeters, Unpublished.
- [11] A. R. de C. Romaguera, M. M. Doria, F. M. Peeters,

Phys. Rev. B 75 (18) (2007) 184525.

[12] Y. N. Ovchinnikov, Sov. Phys. JETP 52 (1980) 775.